Nano Progress

Ariviyal Publishing

Research Article

DOI: 10.36686/Ariviyal.NP.2022.04.07.035

Nano Prog., (2022) 4(7), 8-13.

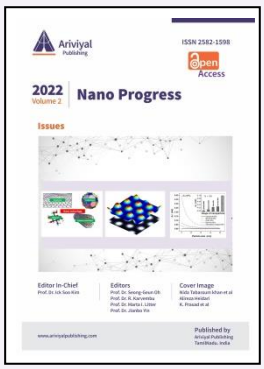

Effect of Sodium Hydroxide Molarity on the Alkali-Activated Fly Ash and Granulated Slag Geopolymer Binders with Water Glass – Part I

H. H. M. Darweesh

Refractories, Ceramics and Building Materials Department, National Research Centre, Cairo, Egypt.

***Corresponding author E-mail address**: hassandarweesh2000@yahoo.com

ISSN: 2582-1598

Crossref

Publication details
Received: 07th March 2022
Revised: 25th May 2022
Accepted: 25th May 2022
Published: 06th June 2022

Abstract: Physical and mechanical properties of the prepared geopolymers composed from granulated blast furnace slag and pulverized flay ash activated with sodium hydroxide and sodium silicates with different molarities of NaOH were investigated. Results showed that the bulk density, flexural and compressive strength improved and enhanced as the molarity of the activator increased till 10 M NaOH, while the total porosity as well as water absorption of the hardened specimens decreased. With any further increase in the molarity of the activator, all these characters were negatively affected, i.e. the water absorption and total porosity rein creased, whereas the bulk density, flexural and compressive strengths diminished. So, the optimum molarity of the activator is 10 M NaOH.

Keywords: Geopolymer; Activator; Molarity; Water Absorption; Porosity; Strength

1. Introduction

Scope of the Problem: The rapid increase in the price of energy made most nations to do their best to optimize its use in order to reduce the related cost burden. Cement is one of the most energy-consuming industries either in thermal or electrical forms. Cement is always used as a binder in the construction technology which has a crucial impact on the quality of materials. Cement industry consumes high energy and discards a high rate of anthropogenic CO_2↑ in the atmosphere, and moreover causes many environmental problems particularly air pollution due to the cement kiln dust waste.[1-5] Recent studies have demonstrated that the partial replacement of cement using supplementary cementitious materials is one of the most promising alternatives to control the production of OPC to minimize the emission of CO_2↑.[6-8] Moreover, the cement industry needs eco-friendly materials to reduce greenhouse gas emission. To achieve this target, it has recently introduced alternative materials as low or no clinker binders like geopolymers to reduce the harmful impacts of cement production on the environment.[9-11] Geopolymers are considered as an environmental-friendly binder because they harden at ambient temperatures and therefore, their synthesis demands less energy depending on the activator up to 80 % less CO_2 emission if compared to ordinary Portland cement.[12–14]

A global trend is the reutilization of industrial waste or by-products in useful applications to maintain environmental balance and public health.[15] Geopolymer is a well-known recent construction material, which was firstly described by Davidovits.[16] Geopolymers can be used in a wide range of potential applications as building materials, fire-resistant and refractory materials, adhesives, binders, low energy ceramics, high-tech resin systems, radioactive, absorbents for removing heavy metals from waste water, thermal insulation and many others.[17-19] The main aluminosilicate precursors for alkali-activated binders are those rich in Al_2O_3 and SiO_2, as in some by-product materials such as fly ash, and granulated ground blast furnace slag.

Geopolymers are the resultant binders generated when aluminosilicate-based materials dissolved in a highly-alkaline medium producing alkali-aluminosilicate-gel, where the main activators are a combination of sodium hydroxide and glassy silicate. Geopolymerization is a chemical reaction performed with silico/aluminates in an alkaline activator, i.e. any source containing SiO_2 and/or Al_2O_3 can be dissolved in an alkaline activator. These reactions are often occurred at high temperatures.[20] There are three steps could be taken place in the process of geopolymerization. The first step is the dissolution of aluminosilicate materials forming polymers-like, which grow and begin to form crystals. The second step is the reorientation of compounds to form gel-like materials.

Table 1. Oxide Analysis of the Starting Raw Materials, wt. %

Oxides	Raw materials	
	GBFS	PFA
L.O.I	0.33	1.81
SiO_2	38.04	52.56
Al_2O_3	5.76	24.85
Fe_2O_3	2.32	9.72
CaO	37.72	5.13
MgO	12.84	1.75
MnO	0.76	----
Na_2O	----	0.56
K_2O	----	2.84
SO_3	0.63	0.38
I.R.	1.60	0.40
Total	100 %	100 %

The third step is the solidification, i.e. the formed gel continuously takes place to finally create semi-crystalline or amorphous three-dimensional aluminosilicate, known as geopolymers.[21,22] During geopolymerization, silico-aluminates can react quickly in an alkaline activator to produce a hardened geopolymer.

Geopolymers give a wide range of applications to provide an opportunity for recycling the huge quantities of industrial waste or by-products, i.e. geopolymers could be produced from waste materials containing large amounts of aluminosilicate. Among these materials fly ash which is one of the most abundantly available industrial wastes. About 900 million tons of fly ash reported to be generated every year.[23,24] China produces the highest amount of fly ash as about 580 million tons yearly, while in India about 170 million tons in the year.[25,26] In USA is around 45 million tons in a year, while it is approximately 14 million tons in Australia each year,[25-27] Granulated blast furnace slag (GBFS), silica fume (SF) and metakaolin.[28-30]

Industrial wastes are extremely hazardous to the environment and all living creatures. Moreover, its disposal is challenging and so expensive, and the legal regulations impose serious responsibilities on the producer. The GBFS/FA geopolymer pastes improved the workability and setting time.[31] The effect of molarity of NaOH on geopolymer pastes containing laterite aggregate having high aluminosilicate content was studied.[32] Although the strength generally decreases at 10 M in traditional geopolymer concrete, the strength of subsequent geopolymer concrete gain has been observed above 16 M. This is due to that the high amount of aluminosilicate in the aggregate acquires the geopolymerization progress at excessive concentration of NaOH.[33]

Objectives of the study: The physical, chemical and mechanical properties of granulated blast furnace slag/fly ash geopolymers activated with different molarity of NaOH (7-12 M) were investigated. Thus, the selected geopolymer at the optimum.

2. Experimental Section

2.1. Raw Materials

The raw materials used in the current study are granulated blast furnace slag (GBFS) and pulverized fly ash (PFA). The GBFS sample, activated by dried sodium silicate (Na_2SiO_3), was supplied by El-Amria

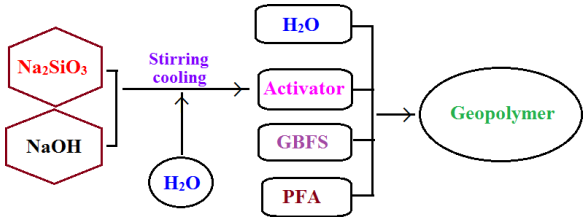

Fig. 1. Preparation Procedures of the Geopolymer

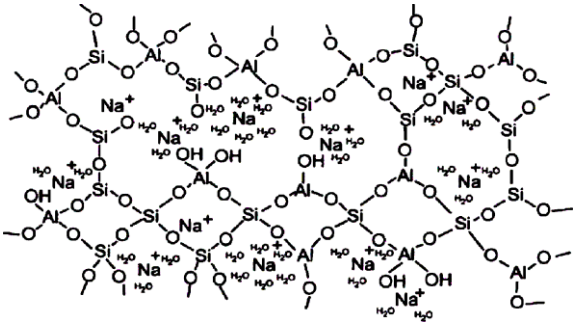

Fig. 2. Schematic Diagrams of the Three-Dimensional Geopolymer Structure.

Fig. 3. A Part of the Polymerization Chain

cement company, Alexandria, Egypt. The PFA sample was taken from the Agricultural Research Centre, Giza, Egypt. The used PFA confirms the ASTM-specification standards.[34] The Blaine surface areas of the raw materials are 5850 and 6100 cm^2/g, respectively. The chemical analysis of the raw materials as performed with X-ray florescence technique (XRF) is listed in Table 1. The NaOH pellets were supplied by EL-Goumhoria chemical company, Ramsis, Cairo, Egypt, while the water glass (WG) was supplied from silica Egypt Company, Burg Al-Arab, Alexandria, Egypt. Water glass (Na_2SiO_3, 26.75% SiO_2, 8.85% Na_2O) and NaOH with the purity of 99.25% were used to prepare the alkaline activator solution. Equation 1 illustrates the basic empirical formula for geopolymer chain.

$$M_n\,[-(SiO_2)z - AlO_2]n.wH_2O \qquad (1)$$

Where, M is the monovalent alkali metal or cation as K^+, Na^+, Ca^{2+}, Li^+ etc. The symbol (-) indicates the presence of a bond, n is the degree of polycondensation or polymerization and z is 1, 2, 3 etc. Fig. 1 demonstrates the preparation procedures of the geopolymer. Fig. 2 shows a schematic diagram of the three-dimensional geopolymer structure.[35] While Fig. 3 illustrated a part of the polymerization chain,[16] respectively.

2.2. Preparation

NaOH solutions were prepared by dissolving the NaOH pellets in distilled water to obtain 7-12 M NaOH solutions. The alkaline activator solution was performed by mixing Na_2SiO_3: 7-12 M NaOH

Table 2. Mix Composition of the Various Geopolymer Pastes, wt. %

Materials Mixes	GBDS	PFA
S1	50	50
S2	50	45
S3	50	40
S4	50	35
S5	50	30
S6	50	25

solutions with the ratio of 1:1 (wt./wt.) noticing that the molarity of the used NaOH solution was taken into consideration. The base batch of the geopolymers binder was prepared from 50 wt % GBFS and 50 wt % PFA. Then, the GBFS was increased at the expense of PFA as 0, 5, 10, 15, 20 and 25 wt. % to study the effect of NaOH molarity on the physical and mechanical properties of the prepared GBFS/PFA geopolymers as shown in Table 2. Then, each alkaline activator solution with different molarities of NaOH was added to the powder composition step by step and well mixed till reach the total homogeneity using a mechanical mixer at the ratio 5:2 of solid materials and activator (wt/wt). The prepared pastes were poured into the molds and pressed at 30 bars for 10 seconds, and at once, it de-molded. They were cured in an oven at 75°C for 24 hours. During the curing process, pastes were kept in furnace to avoid the loss of moisture content.

2.3. Methods

The GBFS and PFA samples were dried to a constant weight in an oven at 105°C to determine the moisture content. Then, it was ignited at 800°C for 50 minutes to calculate the loss on ignition (LOI).

$$MC, \% = A/B \times 100 \quad (2)$$

$$LOI, \% = D - E/D - C \times 100 \quad (3)$$

Where, MC is the moisture content, %, A is the mass loss, g, B is the initial mass, g, C is the mass of empty crucible, g, D is the mass of the moisture-free material and crucible, g, and E is the mass of ignited material and crucible, g.

The water absorption, %, bulk density, g/cm^3 and total porosity, % [37,38] of the hardened geopolymer pastes were calculated according the following equation:

$$WA, \% = (W1 - W2)/(W3) \times 100 \quad (4)$$

$$BD, g/cm^3 = (W3)/(W1 - W2) \quad (5)$$

$$\delta, \% = (W1 - W3)/(W1 - W2) \times 100 \quad (6)$$

Where, δ is the total porosity, W1 is the saturated weight, W2 is the suspended or submerged weight and W3 is the dry weight, respectively.

Flexural strength, MPa[39-41] of geopolymer was conducted using a simple beam with three loading point system Universal testing machine. The test was performed on rectangular prism samples, with 10 mm width, 70 mm length and 10 mm thickness. The spam distance between the two supports was 50 mm. The test was undertaken at a cross-head speed of 1 mm/min. Each test was carried out in triplicate and the value was considered. The flexural strength could be calculated from the following equation:

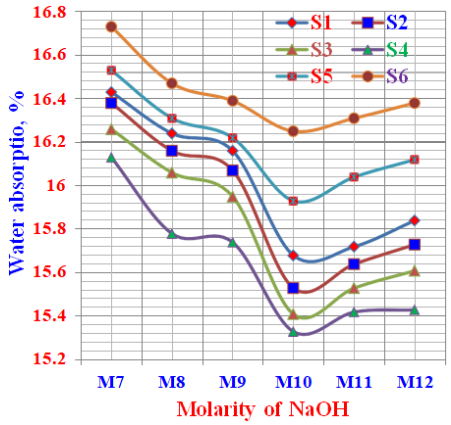

Fig. 4. Water Absorption of the Prepared Hardened Geopolymer Pastes According to the Activator Molarity of NaOH

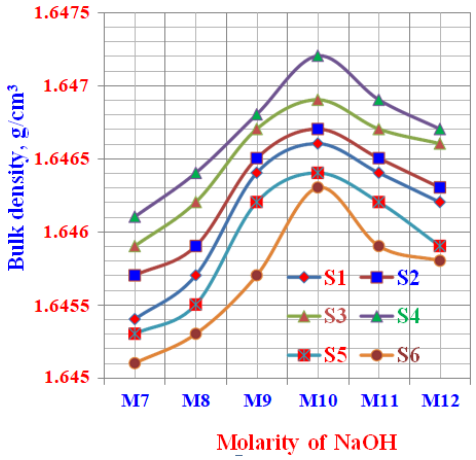

Fig. 5. Bulk Density of the Prepared Hardened Geopolymer Pastes According to the Activator Molarity of NaOH

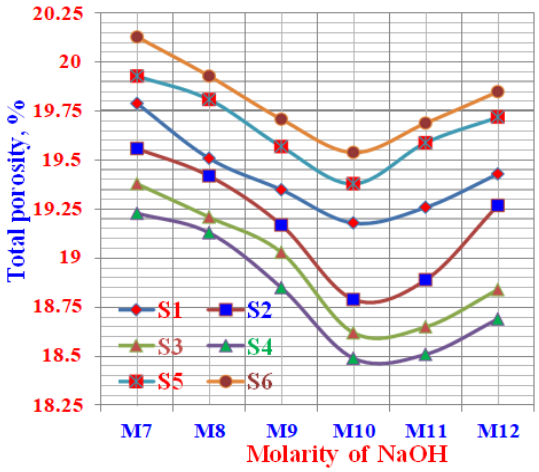

Fig. 6. Total Porosity of the Prepared Hardened Geopolymer Pastes According to the Activator Molarity of NaOH

$$FS, \text{MPa} = 3(L \times S)/2 \ (W \times T^2)/2 \ \ kg/cm^2/10.2 \quad (7)$$

Where, FS is the flexural strength (MPa), F is the maximum load (N), L is the distance between the two supports (mm), B is the width (mm), H is the thickness (mm).

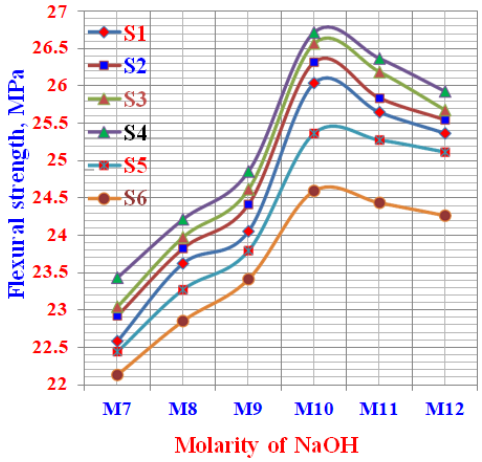

Fig. 7. Flexural Strength of the Prepared Hardened Geopolymer Pastes According to the Activator Molarity of NaOH

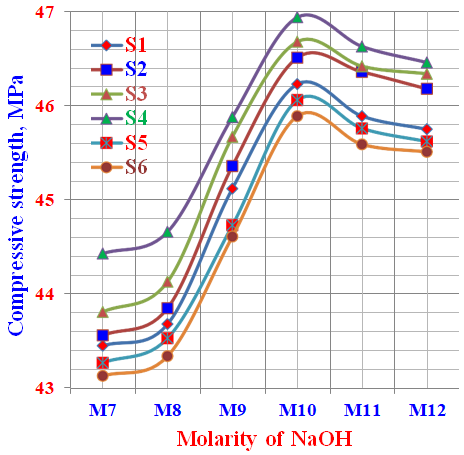

Fig. 8. Compressive Strength of the Prepared Hardened Geopolymer Pastes According to the Activator Molarity of NaOH

Compressive strength, MPa[41-44] was measured by Universal testing machine, operating with a cross-head speed of 2 mm/min. The test was performed on cylindrical samples, with a diameter of 20 mm and a height of 30 mm. Each test was carried out in triplicate, and the average was taken. The compressive strength could be determined by the following relation:

$$CS, \text{MPa} = (D)/(L) \times (W) = kg/cm^2/10.2 \quad (8)$$

Where, CS is the compressive strength kg/cm^2, D is the load, kg, $\boldsymbol{L}$ and $\boldsymbol{W}$ is the length and width of the samples, respectively.

3. Results and Discussions

3.1. Water absorption, bulk density and total porosity

The water absorption, bulk density and total porosity of the prepared activated hardened geopolymer pastes are graphically plotted as a function of NaOH molarity in Figs. 4-6, respectively. As it is clear, the bulk density of the various geopolymers improved and increased with the molarity of the activator till 10 M. Also, the bulk density improved and enhanced too as the ratio of GBFA increased at the expense of PFA. This is mainly attributed to the fact that the density of GBFS is much higher than those of PFA.[15-19] With any further increase in the molarity of NaOH activator, all the previously mention properties were adversely affect. Therefore, the optimum molarity of the activator is 10 M.[10-16,34-38] As a result, the prepared geopolymers became denser, less porous, and less absorbent. This is mainly due to the very fine particle size distribution of initial raw materials.[45-47] Though the great water absorption values and lower bulk densities of geopolymers S5 and S6, it is a promising for the production of porous geopolymers.

3.2. Water absorption, bulk density and total porosity

Fig. 7 shows the flexural strength of the various geopolymer mixes as a function of NaOH molarity. It is obvious that the flexural strength values improved and increased as the molarity of the NAOH activator increased till reach to 10 M. This is essentially contributed to the composition of each geopolymer, in addition the activation effect of the activator.[15,23,37,38] With any further increase in the activator molarity, the flexural strength was affected adversely and decreased. This may be firstly attributed to the large deficiency of the very fine particles reacted of PFA besides to the aid of the defect occurred by the high molarity of the activator.[27,39,40] Consequently, the optimum molarity of the activator is 10 M.[10-16,33-38] Many experimental studies have reported that it was appropriate to use 10 M NaOH for the geopolymerization process.[37,48-50] Some investigators[51-53] concluded that the best results were obtained with 10 M NaOH.

3.3. Compressive Strength

The compressive strength of the various geopolymer pastes is graphically plotted as a function of NaOH molarity in Fig. 8. The compressive strength of the various hardened geopolymer pastes enhances and improved with increase of the molarity of the activator, i.e. as the NaOH molarity increased, the compressive strength accordingly increased too. This is principally due to the variability of the constituents of the geopolymers, in addition the large positive effect of the activator.[16,21,37] The highest compressive strength was obtained with 10 M activator for all geopolymer mixtures at which the non or the least quantity of the unreacted particles with the activator solution.[38,54-56] The unreacted PFA particles negatively affected the mechanical properties of the geopolymer. Hence, this can explain why the high GBFS containing geopolymer has higher mechanical properties than the high PFA containing ones.[54-56] It is an advantage of using more GBFA to improve the geopolymerization process.[16,21,37,45] Furthermore, the chemical composition of GBFS where high ingredient of SiO_2, Al_2O_3, Fe_2O_3 and the low CaO content of this material help to improve and enhance this process. With the further increase of the activator, the compressive strength, but even all the physical properties were often adversely affected.

3.4. Mechanism of geopolymerization

Geopolymerization reacting process usually occurs in three reaction stages: Dissolution– Coagulation, Coagulation–Condensation, Condensation–Polymerization.[23,57] The first stage is Dissolution–Coagulation where the reaction begins with the breakage of siloxane

(Si–O–Si) ions with OH- ions from the alkali activating solution to yield silanol (–Si–OH) and sialate (-Si- O-) types. The presence of alkali cations normalizes the negative charge while the formation of Si–O–Na+ bond hinders the reversion to siloxane.[23,58] The OH- ions also impacts the Si–O– Al bond in the same way forming complex kinds, of majorly Al (OH)4- anions.[58] Dissolution step depends on the temperature, pH- value and the possible treatments of the source materials. The higher fineness and higher pH values favours the dissolution step forming monomeric aluminate and silicate units.[23,59] In the 2nd stage, the assemblage of ionic species helps to generate contact among the disaggregated products and poly-condensation starts causing an increase in the coagulated structure. The silica monomers interact to form dimers and then converted to polymers. In the 3rd stage, the further reaction products precipitated due to the presence of particles in the initial solid phase forming three dimensional polymeric chain and ring structures consisting of Si–O–Al–O bonds. However, the three stages may be overlapped with each other and occurred almost simultaneously. This made it difficult to isolate and examine each of them separately.[21,23,58–63]

4. Conclusions

An environmentally-friendly solution was carried out by using of GBFS and PFA waste materials to produce geopolymer which is too interesting to reduce its hazardous influence and to avoid the difficulties of its storage. This study investigated the effect of the alkaline molarity of the activator on the physical and mechanical properties of GBFS/PFA based geopolymers. Initially, increasing the concentration or molarity of the alkaline activator, NaOH improved and increased of all physical and mechanical properties. The bulk density, flexural and compressive strengths improved and enhanced with the increase of the molarity of NaOH activator only up to 10 M. It is therefore the most suitable concentration for the preparation of GBFA/PFA- based geopolymers. With any further increase of the alkalinity or molarity of the activator more than 10 M, all physical and mechanical properties were adversely affected. The geopolymer containing 65 wt. % GBFS and 35 wt. % PFA (S4) achieved the highest bulk density, flexural and compressive results, and moreover the lowest water absorption and total porosity, and the optimum molarity of the NaOH activator is 10 M.

Acknowledgements

Authors wish to express their deep thanks for National Research Centre for helping to obtain materials, processing, preparing, molding and measuring all of the obtained data of the study.

Conflicts of Interest

The author declares no conflict of interest.

References

1 Mikulcic H.; Klemes J.J.; Vujanovic M.; Urbaniec K.; Duic N. Reducing Greenhouse Gasses Emissions by Fostering the Deployment of Alternative Raw Materials and Energy Sources in the Cleaner Cement Manufacturing Process. *J. Clean. Prod*., 2016, **136**, 119-132. [CrossRef]
2 Miller S.A.; John V.M.; Pacca S.A.; Horvath A. Carbon Dioxide Reduction Potential in the Global Cement Industry by 2050. *Cem. Concr. Res*., 2018, **114**, 115-124. [CrossRef]
3 Darweesh H.H.M.; Wahsh M.M.S.; Negim E.M. Densification and Thermomechanical Properties of Conventional Ceramic Composites Containing Two Different Industrial Byproducts. *Am.-Eurasian J. Sci. Res*., 2012, **7**, 123-130. [Link]
4 Darweesh H.H.M. A Review Article on the Influence of the Electrostatic Precipitator Cement Kiln Dust Waste on the Environment and Public Health. *Am. J. Biol. Environ. Stat*., 2017, **3**, 36-43. [Link]
5 Darweesh H.H.M. Ceramic Wall and Floor Tiles Containing Local Waste of Cement Kiln Dust—Part I: Densification Parameters. *Am. J. Environ. Eng. Sci*., 2015, **2**, 35-43. [Link]
6 Krishnya S.; Yoda Y.; Elakneswaran Y. A Two-Stage Model for the Prediction of Mechanical Properties of Cement Paste. *Cem. Concr. Compos*., 2021, **115**, 103853. [CrossRef]
7 Krishnya S.; Elakneswaran Y.; Yoda Y. Proposing a Three-Phase Model for Predicting the Mechanical Properties of Mortar and Concrete. *Mater. Today Commun*., 2021, **29**, 102858. [CrossRef]
8 Krishnya S.; Herath C.; Elakneswaran Y.; Gunasekara C.; Law D.W.; Setunge S. Modeling of Hydration Products and Strength Development for High-Volume Fly Ash Binders. *Constr. Build. Mater*., 2022, **320**, 126228. [CrossRef]
9 Darweesh H.H.M. Gradual Glass Waste Replacement at the Expense of Feldspar in Ceramic Tiles. *J. Build. Pathol. Rehabilitation*, 2021, **6**, 1-10. [CrossRef]
10 Provis J.L. Alkali-Activated Materials. *Cem. Concr. Res*., 2018, **114**, 40-48. [CrossRef]
11 Gartner E.; Sui T. Alternative Cement Clinkers. *Cem. Concr. Res*., 2018, **114**, 27-39. [CrossRef]
12 Proano L.; Sarmiento A.T.; Figueredo M.; Cobo M. Techno-Economic Evaluation of Indirect Carbonation for CO_2 Emissions Capture in Cement Industry: A System Dynamics Approach. *J. Clean. Prod*., 2020, **263**, 121457. [CrossRef]
13 Tailby J.; MacKenzie K.J. Structure and Mechanical Properties of Aluminosilicate Geopolymer Composites with Portland cement and its Constituent Minerals. *Cem. Conc. Res*., 2010, **40**, 787-794. [CrossRef]
14 Villa C.; Pecina E.T.; Torres R.; Gomez L. Geopolymer Synthesis using Alkaline Activation of Natural Zeolite. *Constr. Build. Mater*., 2010, **24**, 2084-2090. [CrossRef]
15 Darweesh H.H.M. Geopolymer Cements from Slag, Fly Ash and Silica Fume Activated with Sodium Hydroxide and Water Glass. *Interceram-Int. Ceram. Rev*., 2017, **66**, 226-231. [Link]
16 Davidovits J. Geopolymer Chemistry and Applications. 5th Edition. *J. Davidovits.–Saint-Quentin, France,* 2020. *[Link]*
17 Mehta A.; Siddique R. Sustainable Geopolymer Concrete using Ground Granulated Blast Furnace Slag and Rice Husk Ash: Strength and Permeability Properties. *J. Clean. Prod*., 2018, **205**, 49-57. [CrossRef]
18 Neville AM. Properties of Concrete, 5th Edn, Longman Essex (UK), 2011. [Link]
19 Hewlett PC.; Liska M. Lea's Chemistry of Cement and Concrete, 5th ed., Edward Arnold Ltd., London, England, 2017. [Link]
20 Medpelli D.; Sandoval R.; Sherrill L.; Hristovski K.; Seo D.K. Iron Oxide-Modified Nanoporous Geopolymers for Arsenic Removal from Ground Water. *Resource-Efficient Technologies*, 2015, **1**, 19-27. [CrossRef]
21 Ling Y.; Wang K.; Li W.; Shi G.; Lu P. Effect of Slag on the Mechanical Properties and Bond Strength of Fly Ash-Based Engineered Geopolymer Composites. *Compos. B. Eng*., 2019, **164**, 747-757. [CrossRef]
22 Banupriya C.; John S.; Suresh R.; Divya E.; Vinitha D. Experimental Investigations on Geopolymer Bricks/Paver Blocks. *Indian J. Sci. Technol*., 2016, **9**, 113-118. [Link]
23 Khale D.; Chaudhary R. Mechanism of Geopolymerization and Factors Influencing its Development: A Review. *J. Mater. Sci*., 2007, **42**, 729-746. [CrossRef]
24 Hameed A.M.; Rawdhan R.R.; Al-Mishhadani S.A. Effect of Various Factors on the Manufacturing of Geopolymer Mortar. *Arch. Sci*., 2017, **1**, 1-8. [Link]
25 Cao V.D.; Pilehvar S.; Salas-Bringas C.; Szczotok A.M.; Do N.B.D.; Le H.T.; Carmona M.; Rodriguez J.F.; Kjoniksen A.L. Influence of Microcapsule Size and Shell Polarity on the Time-Dependent Viscosity

of Geopolymer Paste. *Ind. Eng. Chem. Res*., 2018, **57**, 9457-9464. [CrossRef]
26 Xie J.; Wang J.; Rao R.; Wang C.; Fang C. Effects of Combined usage of GGBS and Fly Ash on Workability and Mechanical Properties of Alkali Activated Geopolymer Concrete with Recycled Aggregate. *Compos. B. Eng*., 2019, **164**, 179-190. [CrossRef]
27 Herath C.; Gunasekara C.; Law D.W.; Setunge S. Performance of High Volume Fly Ash Concrete Incorporating Additives: A Systematic Literature Review. *Constr. Build. Mater*., 2020, **258**, 120606. [CrossRef]
28 Yang J.; Huang J.; Su Y.; He X.; Tan H.; Yang W.; Strnadel B. Eco-Friendly Treatment of Low-Calcium Coal Fly Ash for High Pozzolanic Reactivity: A Step towards Waste Utilization in Sustainable Building Material. *J. Clean. Prod*., 2019, **238**, 117962. [CrossRef]
29 Moghaddam F.; Sirivivatnanon V.; Vessalas K. The Effect of Fly Ash Fineness on Heat of Hydration, Microstructure, Flow and Compressive Strength of Blended Cement Pastes. *Case Stud. Constr. Mater*., 2019, **10**, 00218. [CrossRef]
30 Zhou Z.; Sofi M.; Lumantarna E.; San Nicolas R.; Hadi Kusuma G.; Mendis P. Strength Development and Thermogravimetric Investigation of High-Volume Fly Ash Binders. *Materials*, 2019, **12**, 3344. [CrossRef]
31 Toniolo N.; Boccaccini A.R. Fly Ash-Based Geopolymers Containing Added Silicate Waste. A Review. *Ceram. Int*., 2017, **43**, 14545-14551. [CrossRef]
32 Wu Y.; Lu B.; Bai T.; Wang H.; Du F.; Zhang Y.; Cai L.; Jiang C.; Wang W. Geopolymer, Green Alkali Activated Cementitious Material: Synthesis, Applications and Challenges. *Constr. Build. Mater*., 2019, **224**, 930-949. [CrossRef]
33 Wan X.; Ren D.; Liu Y.; Fu J.; Song Z.; Jin F.; Huo Z. Facile Synthesis of Dimethyl Succinate Via Esterification of Succinic Anhydride over ZnO in Methanol. *ACS Sustain. Chem. Eng*., 2018, **6**, 2969-2975. [CrossRef]
34 Song W.; Zhu Z.; Peng Y.; Wan Y.; Xu X.; Pu S.; Song S.; Wei Y. Effect of Steel Slag on Fresh, Hardened and Microstructural Properties of High-Calcium Fly Ash Based Geopolymers at Standard Curing Condition. *Constr. Build. Mater*., 2019, **229**, 116933. [CrossRef]
35 Rowles M.R.; Hanna J.V.; Pike K.J.; Smith M.E.; O'connor B.H. 29Si, 27Al, 1H and 23Na MAS NMR Study of the Bonding Character in Aluminosilicate Inorganic Polymers. *Appl. Magn. Reson*., 2007, **32**, 663-689. [CrossRef]
36 Davidovits J. Geopolymer. *Chemistry and Applications. Institute Geopolymere, Saint-Quentin*, France, 2008.
37 Mathew G.; Issac B.M. Effect of Molarity of Sodium Hydroxide on the Aluminosilicate Content in Laterite Aggregate of Laterised Geopolymer Concrete. *J. Build. Eng*., 2020, **32**, 101486. [CrossRef]
38 KOCKAL N.; Beycan O.; Gulmez N. Physical and Mechanical Properties of Silica Fume and Calcium Hydroxide Based Geopolymers. *Acta Phys. Pol. A*, 2017, **131**. [CrossRef]
39 ASTM-C618. *Standard Specification for Coal Fly Ash and Raw or Calcined Natural Pozzolan for Use in Concrete*, ASTM International, West Conshohocken, PA, 2019. [Link]
40 Khater H.M. Hybrid Slag Geopolymer Composites with Durable Characteristics Activated by Cement Kiln Dust. *Constr. Build. Mater*., 2019, **228**, 116708. [CrossRef]
41 ASTM-C373-14a. *Standard Test Method for Water Absorption, Bulk Density, Apparent Porosity, and Apparent Specific Gravity of Fired Whiteware Products, Ceramic Tiles, and Glass Tiles*, West Conshohocken, PA, 2014. [Link]
42 ASTM C. 78-02. *Standard Test Method for Flexural Strength of Concrete (Using Simple Beam with Third-Point Loading)*. 2002. [Link]
43 Darweesh H.H.M. Ceramic Wall and Floor Tiles Containing Local Waste of Cement Kiln Dust—Part II: Dry and Firing Shrinkage as well as Mechanical Properties. *Am. J. Civ. Eng. Archit*., 2016, **4**, 44-49. [Link]
44 ASTM C773-88. *Standard Test Method for Compressive (Crushing) Strength, of Fired White ware Materials*, West Conshohocken, PA, 2011. [Link]
45 Darweesh H.H.M. Nanomaterials: Classification and Properties-Part I. *J. Nanosci*., 2018, **1**, 1-11. [Link]
46 Darweesh H.H.M. Nanoceramics: Materials, Properties, Methods and Applications—Part II. *J. Nanosci*., 2018, **1**, 40-66. [Link]
47 Darweesh H.H.M. Characteristics of Portland cement Pastes Blended with Silica Nanoparticles. *Chem. J*., 2020, **5**, 1-14. [Link]
48 Darweesh H.H.M. Utilization of Nano-Grain Size Particles of Natural Perlite Rock in Blended Cement-Part II: Durability against Sulfate Attack. *Research & Development in Material Science*, 2020, **14**, 1512-1519 [Link]
49 Phoo-ngernkham T.; Maegawa A.; Mishima N.; Hatanaka S.; Chindaprasirt P. Effects of Sodium Hydroxide and Sodium Silicate Solutions on Compressive and Shear Bond Strengths of FA–GBFS Geopolymer. *Constr. Build. Mater*., 2015, **91**, 1-8. [CrossRef]
50 Kourti I.; Rani D.A.; Deegan D.; Boccaccini A.R.; Cheeseman C.R. Production of Geopolymers using Glass Produced from DC Plasma Treatment of Air Pollution Control (APC) Residues. *J. Hazard. Mater*., 2010, **176**, 704-709. [CrossRef]
51 Jaya N.A.; Yun-Ming L.; Abdullah M.M.A.B.; Cheng-Yong H.; Hussin K. March. Effect of Sodium Hydroxide Molarity on Physical, Mechanical and Thermal Conductivity of Metakaolin Geopolymers. In IOP Conference Series: *Mater. Sci. Eng*., 2018, **343**, 012015. IOP Publishing. [Link]
52 Hwang C.L.; Huynh T.P. Effect of Alkali-Activator and Rice Husk Ash Content on Strength Development of Fly Ash and Residual Rice Husk Ash-Based Geopolymers. *Constr. Build. Mater*., 2015, **101**, 1-9. [CrossRef]
53 Zahid M.; Shafiq N.; Razak S.N.A.; Tufail R.F. Investigating the Effects of NaOH Molarity and the Geometry of PVA Fibers on the Post-Cracking and the Fracture Behavior of Engineered Geopolymer Composite. *Constr. Build. Mater*., 2020, **265**, 120295. [CrossRef]
54 Zhang M.; El-Korchi T.; Zhang G.; Liang J.; Tao M. Synthesis Factors Affecting Mechanical Properties, Microstructure, and Chemical Composition of Red Mud–Fly Ash Based Geopolymers. *Fuel*, 2014, **134**, 315-325. [CrossRef]
55 Darweesh H.H.M. Low Heat Blended Cements Containing Nanosized Particles of Natural Pumic Alone or in Combination with Granulated Blast Furnace Slag. *Nano Prog*., 2021, **3**, 38-46. [Link]
56 Darweesh H.H.M. Nano-Glass Waste Substitution for Portland cement Pastes. *Nano Prog*., 2021, **3**, 51-59. [Link]
57 Duxson P.; Fernández-Jiménez A.; Provis J.L.; Lukey G.C.; Palomo A.; Van Deventer J.S. Geopolymer Technology: The Current State of the Art. *J. Mater. Sci*., 2007, **42**, 2917-2933. [CrossRef]
58 Pacheco-Torgal F.; Labrincha J.; Leonelli C.; Palomo A.; Chindaprasit P. eds. *Handbook of Alkali-Activated Cements, Mortars and Concretes*. Elsevier. 2014. [Link]
59 Provis J.L.; Van Deventer J.S.J. eds. *Geopolymers: Structures, Processing, Properties and Industrial Applications*. Elsevier, 2009. [Link]
60 Provis J.L.; van Deventer J.S.J. Alkali Activated Materials, State-of-the-Art Report, RILEM TC 224-AAM, *Springer*, Dordrecht Heidelberg New York London, 2014. [Link]
61 Zhang S.; Li V.C.; Ye G. Micromechanics-Guided Development of a Slag/Fly Ash-Based Strain-Hardening Geopolymer Composite. *Cem. Concr. Compos*., 2020, **109**, 103510. [CrossRef]
62 Nematollahi B.; Sanjayan J.; Qiu J.; Yang E.H. Micromechanics-Based Investigation of a Sustainable Ambient Temperature Cured One-Part Strain Hardening Geopolymer Composite. *Constr. Build. Mater*., 2017, **131**, 552-563. [CrossRef]
63 Cai J.; Li X.; Tan J.; Vandevyvere B. Thermal and Compressive Behaviors of Fly Ash and Metakaolin-Based Geopolymer. *J. Build. Eng*., 2020, **30**, 101307. [CrossRef]